Urban Climate 48 (2023) 101402

Contents lists available at ScienceDirect

Urban Climate

journal homepage: www.elsevier.com/locate/uclim

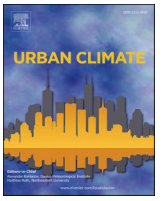

A disaster-damage-based framework for assessing urban resilience to intense rainfall-induced flooding

Xiwen Zhang [a], Feng Mao [b,*], Zhaoya Gong [c,d], David M. Hannah [d], Yunnan Cai [a], Jiansheng Wu [c]

[a] School of Architecture and Urban Planning, Guangdong University of Technology, Guangzhou 510090, China
[b] Institute for Global Sustainable Development, University of Warwick, Coventry CV4 7AL, United Kingdom
[c] School of Urban Planning and Design, Peking University, Shenzhen 518055, China
[d] School of Geography, Earth and Environmental Sciences, University of Birmingham, Birmingham B15 2TT, United Kingdom

ARTICLE INFO

Keywords:
Resilience assessment
Urban resilience
Disaster
Urban flooding
Climate adaptation
Depth-damage curve

ABSTRACT

Resilience has been widely used as a concept to analyse, understand, and improve cities' coping capacities to disasters. However, it is still a challenge to operationalise and quantify resilience. This study proposes a framework for assessing resilience to disasters based on the relationship between disaster intensity and damage rate. We use intense (short-term heavy) rainfall-induced urban flooding in Shenzhen city, one of the largest cities in China, as an example to explore the main features and transferability of the proposed resilience assessment framework. In addition, we demonstrate the usability of the proposed framework by using it to assess and compare the effectiveness of two resilience-building strategies: (1) permeable pavement transformation and (2) land vulnerability reduction. This research makes an innovative contribution through its effective disaster-damage-based approach for quantitatively evaluating urban resilience to disasters, which can support building resilience and mitigating the impact of climate change.

1. Introduction

Climate change has increased the frequency and intensity of extreme weather-related events (Jin et al., 2020; World Bank Group, 2015). Short-term heavy rainfalls and their triggered disasters, such as flooding, pose a threat to the security and sustainable development of human society, especially in urban areas. Moreover, along with the accelerated process of urbanisation, the proportion of impervious areas is gradually increasing, resulting in an increased risk of rainfall-induced flooding, particularly in city centres (Bayazit et al., 2020; Mustafa et al., 2018). Therefore, urban disaster prevention and control have attracted much attention, and improving the ability to deal with extreme disaster events has become an urgent issue to solve.

In the context of climate change, the concept of resilience has gained popularity in guiding disaster risk reduction practices (Munawar et al., 2021; Vachette, 2017; Watson, 2016; Burton et al., 2019). Resilience refers to the capabilities of a system to respond to transient disturbances, shocks, or long-term changes and uncertainties (Field et al., 2012; United Nations Office for Disaster Risk Reduction, 2009). It emphasises the self-organising processes of systems in response to disasters. More specifically, resilience is reflected in the processes such as absorbing damage, adapting to risks, limiting further expansion of disasters when recovering from disasters, and mitigating the impact (Serre and Barroca, 2013; Nelson et al., 2007; Newman et al., 2009; McLellan et al., 2012; Hosseini

* Corresponding author.
E-mail address: Feng.Mao@warwick.ac.uk (F. Mao).

https://doi.org/10.1016/j.uclim.2022.101402
Received 17 May 2022; Received in revised form 9 December 2022; Accepted 22 December 2022
Available online 16 January 2023

and Barker, 2016; Tanner et al., 2017; Vugrin et al., 2011).

In recent years, research communities have heightened focus on intense rainfall events, which are disasters with large amounts of precipitation occurring over a relatively short duration (Tian et al., 2019; Yamagishi et al., 2013). Moreover, floods and geological disasters (e.g., landslides and debris flow) can be caused by intense rainfall events, resulting in extensive loss of property and human life. Therefore, quantitative approaches are needed to assess, build, and manage resilience to intense rainfall. However, operationalising resilience to disasters, especially short-term and heavy precipitation events, and their consequent flooding (enhanced in urban environments with 'hard' built surfaces of low water permeability), has always been a challenge (Yang et al., 2021).

In order to address this challenge, this study proposes a framework for quantitatively assessing resilience to disasters, which is built upon the relationship between the intensive rainfall-induced flood disaster and its damage to urban systems. The aim is supported by three objectives. Firstly, we justify the necessity of proposing this new disaster-damage-based framework for assessing urban resilience by reviewing the literature. Secondly, we explain the rationale and design of the proposed framework. Thirdly, we demonstrate the main features and transferability of the framework by taking the central urban area of Shenzhen city, one of the largest cities in China, as a study area, assessing Shenzhen's resilience to short-term heavy rainfall and urban flooding, and comparing different resilience-building strategies.

The rest of the paper is organised as follows. Section 2 presents an overview of prior work on resilience and its assessment methods. Section 3 introduces the disaster-damage-based framework for assessing urban resilience to disasters with a "disaster intensity – damage rate" curve. Section 4 describes the study area (i.e., central Shenzhen), the data used in this study, and the proposed resilience assessment method. Section 5 shows the results of the urban flooding simulation and Shenzhen's resilience with the disaster damage curve. In Section 6, we compare two resilience-building strategies to demonstrate the usability of the proposed framework, discuss the framework's features, and analyse research uncertainties and future opportunities. The paper concludes in Section 7 with a summary of the framework's contribution as well as potential future work for resilience assessment.

2. A brief overview of current resilience assessment methods

Initially introduced in ecology, the application of resilience has expanded to other fields, including cities, social, and economic systems (Evans, 2011; Hosseini et al., 2016; Mao et al., 2017; Nan and Sansavini, 2017; Wilkinson, 2021; Yang et al., 2019), covering topics such as urban adaptation to climate change, natural disasters, environmental pollution, human conflict, and disease transmission (Jabareen, 2013; Leichenko, 2012; Sapountzaki, 2012; Nunes et al., 2019; Tyler and Moench, 2012). Timmerman (1981) first put forward the interpretation of resilience in the field of climate change research, that is, the ability to absorb disasters and recover from the impact of disasters. The concept of resilience has been widely used for disaster management (Cutter et al., 2008; Hernantes et al., 2017; Keating et al., 2017; Saja et al., 2019). This concept emphasises the process and capabilities that systems, communities or societies deal with and adapt to external shocks and interference and recover from them (United Nations Office for Disaster Risk Reduction, 2009). Disaster resilience is based on the premise that the system has a stable state and strives to maintain or recover to the stable state when it encounters disturbances (Lee, 2019; Dessavre et al., 2016; Manyena et al., 2011). Thus, resilience has become one of the most popular theories in the field of disaster, crisis, and risk research, and research on building resilient cities to cope with climate change and exploring sustainable development of cities has been increasingly recognised by researchers and policymakers.

Based on the theoretical advances of the resilience concept, many assessment methods have been developed to evaluate and analyse resilience in cities or communities, such as index systems (Jabareen, 2013; Cutter and Derakhshan, 2018; ARUP, 2015; STAR COMMUNITIES, 2020), system function curves (Bruneau et al., 2003; Feofilovs and Romagnoli, 2020; Henry and Ramirez-Marquez, 2012; FEMA/NIBS, 2015), and quantitative modelling (NHERI, 2018; SIM·CI, 2018; SAVI, 2020). Among them, index-based resilience assessment is the most used method (Rockefeller Foundation, ARUP, 2014; Sharifi and Yamagata, 2016). This method is suitable for comprehensive resilience evaluation. It evaluates systemic resilience by integrating the performance of subsystems, such as ecosystem, built environment, socioeconomics, management, education, and infrastructure (Birkmann, 2006; De Groeve et al., 2013; Kabir et al., 2018; Sajjad et al., 2021). However, these index systems usually assume a better subsystem condition (e.g., higher biodiversity, wealthier society, and more investment in education) automatically leads to resilience. However, although index systems are relatively simple and easy to operate, they can be highly subjective. For example, given the different understandings of resilience and the variability of objectives across regions, institutions, researchers and policymakers, the resilience index systems and factor weights may differ significantly.

System function curves are commonly used to evaluate resilience quantitatively (Polin and Kane, 2021; Gasser et al., 2021; Murdock et al., 2018). This method regards resilience as a process and quantifies resilience by analysing the impact of disasters on systems and systems' consequent responses (Bruneau et al., 2003; Reed et al., 2009; Cimellaro et al., 2010; Bozza et al., 2017). It describes the change of system function state in the whole process of a single disaster event's occurrence, development, and extinction, and quantifies resilience by calculating the area enclosed by the system function curve and coordinate axes. This method is mainly used for assessing urban infrastructure's resilience to a specific type of disaster, in contrast to the index system's general focus. Although this method provides a helpful perspective for quantitative assessments of resilience, it has limitations. For example, it focuses on assessing the performance under single events rather than disaster patterns, which does not entirely capture the concept of resilience as systemic attributes and capacities. In addition, this method requires a time series of systemic performance data at different disaster stages, which makes data collection and index calculation relatively complex.

Many resilience assessment models have been developed based on the above two categories of methods, by assessing the risk of each component of the system or describing the process of disasters (Tong, 2021; Cheng et al., 2022). In addition, these models consider the factors that affect the system's ability to cope with risk, recover from it, and learn and innovate. For example, Ouyang

et al. (2012) and Mugume et al. (2015) developed quantitative models based on the relationship between a system's function and its disaster damage in single disaster events. They proposed to quantify resilience by assessing the system's functional damage caused by disasters; for example, under a certain level of disasters, a smaller system damage suggesting a greater resilience.

Although many methods have been put forward for resilience assessment, as shown above, further development is needed for a few reasons. For example, most current research on resilience assessment is still confined to conceptual discussions, focusing on the resilience connotation, mechanism and process, and construction of index systems. The implication of the assessment to policymaking, actions, and resilience building is not always clear. In addition, some of the indexes are difficult to be quantified, thus there is not an abundant number of empirical studies on quantifying resilience. Furthermore, regionally different and subjective assessments of resilience make it challenging to compare resilience across regions. In order to respond to these challenges, this study proposes a framework that facilitates quantitative resilience assessment across regions, enables analysis of resilience dynamics, and supports follow-up actions for resilience building.

3. A disaster-damage-based framework for assessing urban resilience to disasters

As reviewed above, resilience describes the system's capacity to cope with and adapt to disturbances and maintain or recover to a stable state. Therefore, resilience can be characterised by the interaction between systems (e.g., urban systems) and their disturbances (e.g., water-related disasters caused by intense precipitation events) (Serre and Barroca, 2013; McLellan et al., 2012; Tyler and Moench, 2012; Adger et al., 2005).

The urban system is a socio-ecological complex system (Restrepo and Morales-Pinzon, 2018; Odum and Odum, 1976; Ongkowijoyo and Doloi, 2018; Irwin et al., 2009). Elements in the urban system interlink closely to ensure its structure and function and achieve a stable state. Urban systems cope with disasters by mobilising internal natural, social, and economic factors to maintain their status and performance and resist damages (Chen et al., 2020a; Chen et al., 2020b; Hajibabaee et al., 2014).

Rainstorms and floods triggered by rainstorms are very common in cities worldwide, and they have aroused extensive attention because of large number of affected people and economic losses. Short-term heavy rainfall is regarded as one of the main disaster-causing factors of urban floods. Therefore, in this study, flooding induced by short-term heavy rainfall is taken as a case of disaster to build the framework for assessing urban resilience.

The impact of disasters on urban systems is usually measured by disaster damage (Meyer et al., 2009), which refers to the loss of all elements of the system in responding to disaster impact after the occurrence of a disaster (Gall, 2015; UNFCCC, 2012). It includes both the direct damage caused by physical or structural impact (e.g., destruction of buildings, properties, infrastructure), and indirect damage caused by reduction or cessation of production, medical expenses, income loss due to nonemployment or impacts on human wellbeing (e.g., casualties, human health) (Cochrane, 2004). The direct damage mainly reflects the system's ability to resist the disaster, and the indirect damage demonstrates its ability to recover from disaster to a stable state. Both types of damage describe the whole process from the occurrence of a disaster to the recovery from it.

The damage is mainly determined by the disaster intensity and the disaster-prone areas' capacity (i.e., resilience) to cope with the disaster. Disaster intensity and damage usually exhibit a non-linear relationship (see Fig. 1). When the intensity of a disaster is low, the urban system is able to absorb disaster's impact and has minimal damage. As the disaster intensity increases and passes a threshold, the damage caused by disasters increases rapidly. With a further increase in disaster intensity, the growth rate of disaster damage slows down. When the intensity of disaster is large enough to destroy an urban system, the disaster damage to the urban system reaches its maximum.

According to the above-described disaster-damage relationship (also see Fig. 1), at a certain disaster intensity level, a higher

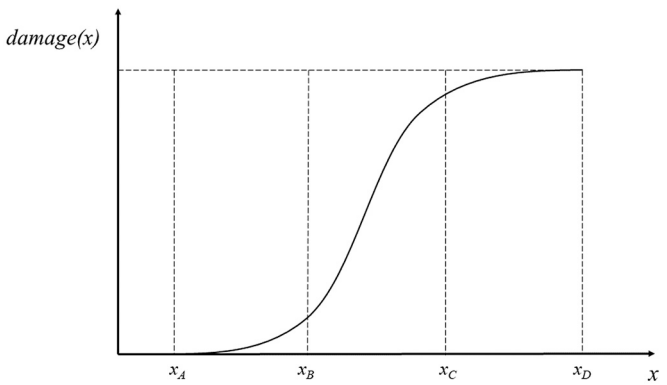

Fig. 1. The conceptual relationship between disaster intensity and disaster damage. x represents the intensity of disasters (e.g., rainfall), and *damage (x)* represents the damage caused by the disaster. In the phase from x_A to x_B, the disaster intensity is minimal compared to the system's coping capacity, and the disaster damage increases slowly along with the increase of disaster intensity. In the phase from x_B to x_C, the disaster intensity is large enough to make disaster damage increase sharply with the increase of rainfall intensity. The disaster-damage relationship in the phase x_C to x_D reaches a stable stage, and the damage is close to the maximum.

damage suggests a lower systemic capacity in coping with disasters, or in other words, a lower level of resilience. Similarly, a higher level of resilience implies the system has the capacity to cope with more intensive disasters without suffering large damage. Examples in Fig. 2 demonstrate different resilience behaviours. The damage to System I increases more rapidly with the growth of the disaster intensity and reaches the maximum damage (y-axis) at a relatively low level of intensity (x-axis). On the contrary, with the increase of disaster intensity, the damage to System II increases more slowly and can withstand heavier rainfall while maintaining the structure and functions of the system. This comparison suggests System II has higher resilience to intense rainfall than System I.

In this study, it is assumed that an urban system has a long-term stable state, which is set as the maximum damage level (Fig. 3). The damage increases along with the growth of the disaster intensity and reaches 100% when the system collapses completely. However, if the system has a higher capacity in coping with disasters, the disaster-damage curve would be flatter or have a gentler slope, implying a larger area above the curve. Therefore, this area enclosed by the disaster-damage curve, the maximum damage line, and the y axis is used as an indicator of resilience (Fig. 3a).

In practice, the disaster-damage curve can be drawn according to the historical disaster data to show the change of a system's damage under the effect of different disaster intensities, and resilience can be measured by the area surrounded by the disaster damage curve and the coordinate axis (see Fig. 3a). However, because the probability of extreme disasters that can completely destroy the urban system is extremely low, we can consider the curve within a certain range of intensity (e.g., x_1-x_2 in Fig. 3b) and damage levels (e.g., 0-d in Fig. 3b). Regarding indicators, the disaster on the x-axis can be measured by variables such as rainfall intensity, or precipitation, and the damage on the y-axis can be indicated by absolute damage or damage rate.

4. Case study's materials and methods

4.1. Study area

In order to demonstrate the proposed urban resilience assessment framework, we choose the central region of Shenzhen city as the research area, and urban flooding induced by short-time heavy rainfall as the research disaster to assess central Shenzhen's resilience to urban flooding.

Shenzhen is a coastal city in south China (113°43′-114°38′E, 22°24′-22°52′N), located in the south of Guangdong Province, on the east bank of the Pearl River Estuary. The total area of Shenzhen city is 1997.47 km^2. The terrain of the whole region is high in the southeast and low in the northwest, and the landform is mainly composed of low hills with a gentle platform between them. The city has a subtropical maritime climate with abundant rainfall of about 1900 mm per year (Li et al., 2015; Zhou et al., 2021), and precipitation increases with thunderstorms, heavy rainstorms, and typhoons. The rainy season is from April to September, and the major flood period is from July to September.

Shenzhen is one of the economic centres in China, with a Gross Regional Product second only to Shanghai and Beijing, ranking the third among mainland cities in 2020. As an example of rapid urbanisation in China, Shenzhen has maintained high intensity and rapid growth. From 1990 to 2019, urban land area has expanded from 139 km^2 to 700 km^2. Thanks to the rapid social and economic development, land use has changed dramatically, leading to a typical urban landscape pattern with impervious surfaces (e.g., buildings and roads) increasing, while natural surfaces (e.g., water areas and green spaces) decreased. A large area has been hardened, which has constantly reduced ecosystem regulation services, leading to the continuous decline of capacity to regulate rainwater, putting significant pressure on the ecological environment and municipal pipe network. However, the construction of drainage systems and supporting facilities are insufficient. For example, the drainage standard of the pipe network is once-in-a-year rainfall, which means drainage pipes are able to resist short-term heavy rainfall events with a return period of one year. It is lower than the defence standards of developed cities in Europe and the United States (e.g., once in five to ten years rainfall), and far lower than the newly revised standard of urban drainage pipe network design "flood-prone areas in megalopolis and megalopolis need to resist once in more than 50 years rainfall" (Jia et al., 2020; Thryse et al., 2018; Ministry of Housing and Urban-Rural Development of the People''s Republic of China, 2014). Shenzhen's imperfect municipal drainage system has been causing flooding problems and damage. For example, a heavy

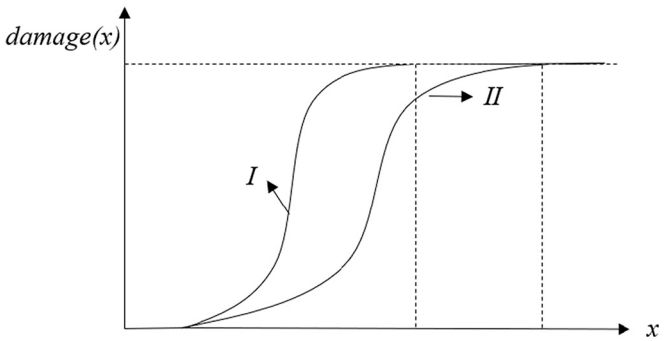

Fig. 2. Two examples of resilience behaviour. In System I, the disaster damage increases rapidly with the increase of disaster intensity. System II is more resilient than System I because System II's disaster damage increases more slowly with the increase of rainfall intensity. At the same rainfall intensity, System II has a lower damage. The x axis denotes the disaster intensity, and the y axis denotes the damage caused by the disaster.

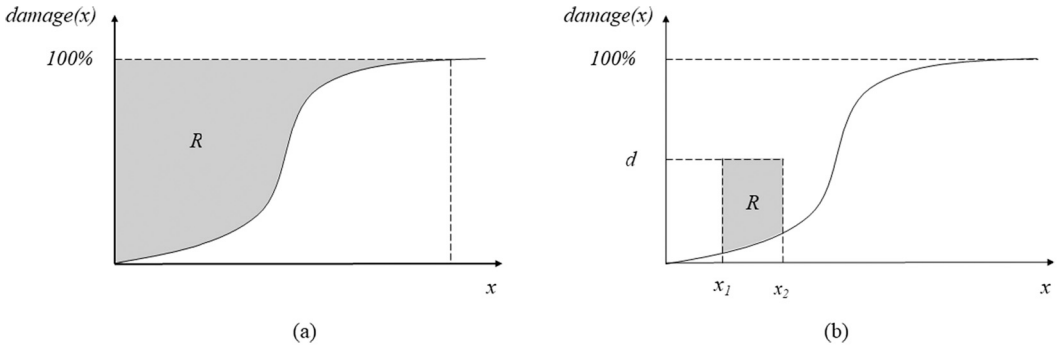

Fig. 3. The proposed framework for assessing resilience. The shaded area, R, enclosed by the disaster-damage curve and the boundaries (i.e., the y-axis or dashed lines) is used to represent resilience. (a) Resilience measured at the full ranges of disaster and damage. (b) Resilience measured at predefined ranges of disaster (x_1 - x_2) and damage (0 - d). The x axis denotes the disaster intensity, and the y axis denotes the damage caused by the disaster.

rainfall event in Shenzhen city on May 11, 2014, caused direct economic damage of nearly 80 million yuan (about USD 523 million).

The central Shenzhen was used for this demonstration, which has an area of 344.88 km^2, accounting for 17.26% of the total area of Shenzhen city (Fig. 4).

4.2. Data

The data used in this study include land use, soil type, Digital Elevation Model (DEM), building distribution data, Point of Interest (POI) data, depth-damage curves, and night-time light data. Urban flooding simulation and resilience assessment were conducted for the year of 2018. If the 2018 data were unavailable, the temporally closest available data were used.

The land use data was from the Finer Resolution Observation and Monitoring of Global Land Cover in 2017 with a spatial resolution of 30 m. There are 10 types of land, namely farmland, forest, grassland, shrub, wetland, waterbody, tundra, construction land, bare land, and snow and ice. The soil type data was from the Harmonized World Soil Database (HWSD) with soil classification system FAO-

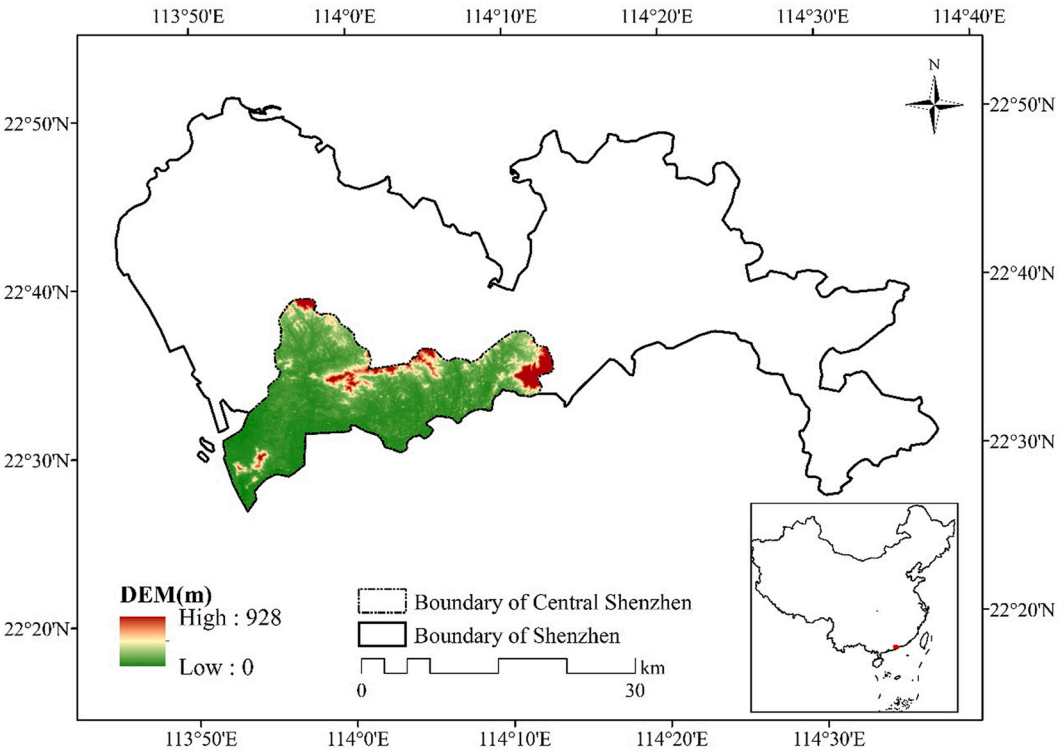

Fig. 4. Location and map of Shenzhen city.

90. The DEM data ASTER-GDEM V2 (2011, spatial resolution of 30 m) was derived from Geospatial Data Cloud (http://www.gscloud.cn/). Building distribution was from the building contour data with variables including building name, address, and height, which was derived from AutoNavi maps in October 2018. In this study, the building height information was superimposed with the original DEM to correct the urban surface elevation. The above data were input into a Soil Conservation Service (SCS) hydrological model for urban flooding simulation.

Point of Interest (POI) was derived from AutoNavi maps (http://ditu.amap.com/), which were obtained by searching for keywords in the "Search POI" API using the Aude Web service. POI data contains basic information such as name, category, coordinates, and street address. POI includes 14 categories, such as shopping service, catering service, life service, company and enterprise, financial and insurance service. Each category was further divided into several sub-categories, such as restaurants, communities, schools, and hotels. This data was used to mark the attribute information of each plot in the study area to identify the types of urban functional land use.

The depth-damage curves were used to describe different land-use's vulnerability to flooding. The European Commission Joint Research Centre (JRC) developed a database of flood inundation depth - disaster damage curves, and these depth-damage curves were produced for each continent (Africa, Asia, North America, South/Central America, Australia, and Europe) according to land-use classes (e.g., residential, commerce, industry, transport, agriculture) (Huizinga et al., 2017). In this dataset, damage is a function of the inundation depth and land-use categories. The value of damage was normalised to 0–1, where 0 represents no damage and 1 represents the maximum damage. The flood depth-damage functions in Asia were used in this study (Huizinga et al., 2017).

In addition, the National Polar-Orbiting Partnership's Visible Infrared Imaging Radiometer Suite (NPP/VIIRS) night-time light data (spatial resolution of 500 m) was from the National Oceanic and Atmospheric Administration National Geophysical Data Center (NOAA/NGDC). This night-time light data is a representation of the intensity of human activities, which has been used to represent socio-economic parameters, such as GDP, population size, and electricity consumption (Agnihotri and Mishra, 2021; Sun et al., 2020; Doll et al., 2006; Sutton et al., 2007; Sun et al., 2021; Jasinski, 2019; Nurbandi et al., 2018; Henderson et al., 2012; Li et al., 2013). In this study, the NPP/VIIRS night-time light data in 2015 was used to represent the land value per unit area, with which the damage of urban flooding disaster was calculated.

4.3. Resilience assessment

According to the proposed resilience assessment framework based on the disaster-damage relationship, this study takes urban flooding as an example to evaluate urban resilience to short-term heavy rainfall by drawing the disaster-damage curve and calculating the shaded area as demonstrated in Fig. 3b. The assessment process includes five steps: (1) setting rainfall scenarios, (2) simulating rainfall-induced urban flooding, (3) evaluating disaster damage, (4) drawing disaster-damage curve, and (5) assessing urban resilience to short-term heavy rainfall (Figure 5).

In the first step, this study set rainfall scenarios based on the historical rainfall characteristics and the Meteorological Bureau's heavy rainfall grading. By comparing the precipitation in 1 h with the maximum cumulative precipitation in a series of durations (2 h,

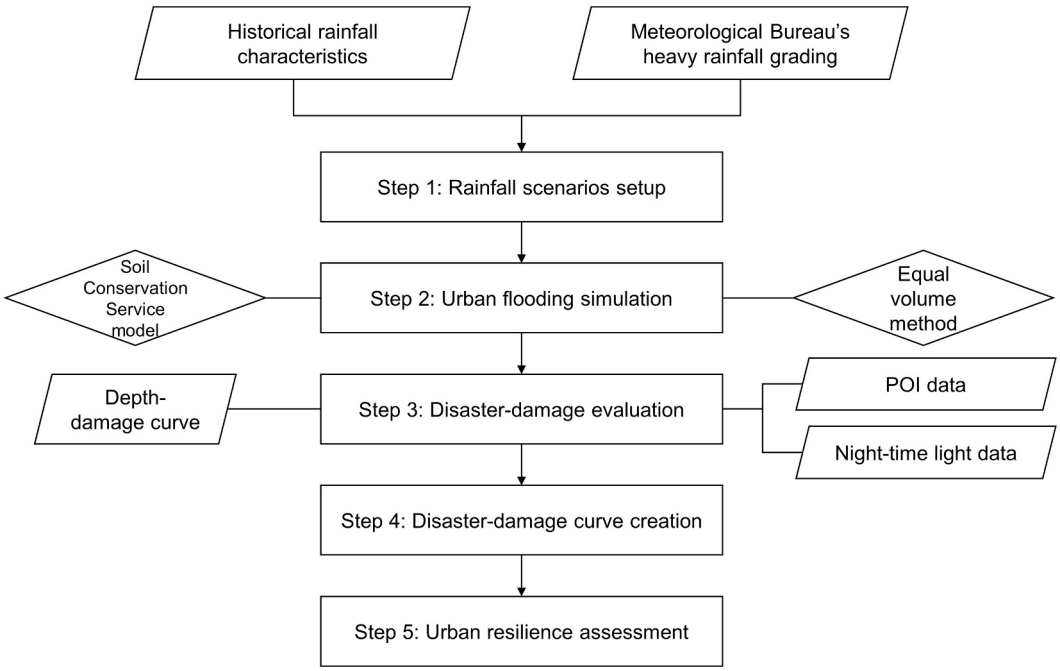

Fig. 5. Flow chart of resilience assessment.

3 h, 4 h, 5 h, 6 h), we found that the maximum cumulative precipitation in 3 h accounts for more than 89.6% of the maximum cumulative precipitation in 6 h, and the precipitation in 1 h accounts for 92% of the cumulative precipitation in 3 h. It can be interpreted that extreme rainfall events in Shenzhen are characterised by high precipitation intensity in short durations (mainly within 1 h). Our pilot flood simulations found that Shenzhen had nearly no inundation areas when the rainfall intensity was lower than 60 mm/h. Based on the hourly rainfall monitoring data from the national meteorological stations in Shenzhen from 1951 to 2018, about 5% of the rainfall events had intensities exceeding 60 mm/h, and the maximum hourly rainfall was 90.5 mm. Therefore, the duration of short-term rainfall was set to 1 h. Rainfall scenarios were 60 mm/h, 65 mm/h, 70 mm/h, 75 mm/h, 80 mm/h, 85 mm/h, 90 mm/h, 95 mm/h and 100 mm/h, covering the most possible range of rainfall intensity causing urban flooding disaster in Shenzhen. Because of the relatively small size of the central urban area and the limited number of national meteorological monitoring stations, we assumed that the rainfall was homogeneous across the study area.

In the second step, urban flooding was simulated using the Soil Conservation Service (SCS) model, which was developed by the United States Department of Agriculture's Soil and Water Conservation Service. The SCS model is an empirical hydrological model that combines rainfall characteristics with local land-use and soil characteristics to determine total surface runoff (United States Department of Agriculture, 1986; Tiwari et al., 2018). Originally designed to estimate runoff in soil and water conservation, the model has been extended to urbanised areas and vegetation-covered river basins. The model has a clear principle and can objectively reflect the influence of different soil types and land cover types on rainfall and runoff. With a simple structure and a small number of input parameters, it is an efficient method to calculate runoff of small watersheds and has been widely used in hydrological research in recent years (Xiao et al., 2011; Verma et al., 2020; Verma et al., 2021; Jahan et al., 2021). Based on the SCS hydrological model and relevant GIS spatial analysis tools, this study built a comprehensive urban flooding model. In this model, urban flooding was regarded as passive inundation. It was assumed that elevation was a key factor affecting the direction of water flow. All grids with elevations lower than the inundation were included in the flooded area. After calculating water accumulating volume in the watersheds and combining with urban DEM, the "equal volume method" was used to simulate the process of urban flooding confluence. Recursive running of the volume analysis was conducted to simulate the depth and spatial distribution of inundation under different rainfall scenarios. According to the "Code for Design of Outdoor Wastewater Engineering (GB 500014-2006)" (Ministry of Housing and Urban-Rural Development of the People's Republic of China (MOHURD), 2016), the inundation depth was divided into six levels: 0–0.5 m, 0.5–1 m, 1–1.5 m, 1.5–2 m, 2–3 m, 3 m above.

In the third step, an indicator of disaster damage rate was constructed to evaluate the relative damage, which was defined as the amount of damage divided by the local GDP. This variable was used to measure the rate of relative (instead of absolute) damage to a city. In central Shenzhen, the total damage rate of the whole city is the ratio of total damage to the total GDP of the city. The damage in a city was calculated as the sum of all the damage of all grid cells in the city, and the damage of each grid cell was the product of the cell's value and its damage rate. The disaster damage rate, D, is calculated as below:

$$D = \frac{\sum_{i=1}^{n} d_i \times V_i}{\sum_{i=1}^{n} V_i} = \sum_{i=1}^{n} d_i \times \frac{V_i}{\sum_{i=1}^{n} V_i} = \sum_{i=1}^{n} d_i \times v_i \tag{1.1}$$

where i is the serial number of grid cells, n is the total number of grid cells in the study area, d_i is disaster damage rate of grid i, V_i is value of grid i, and v_i is the ratio of the value of grid i to the total value of the study area.

In this study, V_i was translated from the light intensity of grid i, considering that night-time light data is a good proxy of socio-economic parameters (Doll et al., 2006; Sutton et al., 2007; Nurbandi et al., 2018; Henderson et al., 2012; Li et al., 2013). It is believed that areas with high brightness of lights is usually a gathering area of human social and economic activities, with high efficiency and economic output of land per unit area, indicating a relatively high level of land value.

The damage rate of the land use type c (d_c) is related to the inundation depth of the cell and the land use type to which the cell belongs:

$$d_c = f_c(Depth) \tag{1.2}$$

where c denotes land use type, *Depth* represents inundation depth of the grid cells, and f_c represents the depth-damage function of land use type c.

Based on the POI data, this study classified the land-use into types by calculating the proportion of each POI in the comprehensive value of all types of POI in each block unit (Xu and Yang, 2017; Chi et al., 2016). Four land use types were produced: residential, commercial, industrial, and transportation lands. Most cells contained multiple land use types and the proportion of each type in each cell was calculated. The damage rate (d_i) of grid cell i can be characterised as follows:

$$d_i = \sum_{c=1}^{4} d_{ic} \times s_{ic} \tag{1.3}$$

where d_{ic} represents the proportion of damage in the land use type c of the grid cell i, and s_{ic} represents the proportion of land use type c in grid cell i.

Therefore, the city's damage rate (D) can be represented as:

$$D = \sum_{i=1}^{n} d_i \times v_i = \sum_{i=1}^{n} \sum_{c=1}^{4} d_{ic} \times s_{ic} \times v_i = \sum_{i=1}^{n} \sum_{c=1}^{4} f_c(Depth) \times s_{ic} \times v_i \tag{1.4}$$

In the fourth step, we took the precipitation as the disaster on the x axis and the damage rate as the damage on the y axis. Based on the damage rate at each precipitation level, scatter points were plotted and connected to form the disaster damage curve.

In the fifth step, built upon the disaster damage rate curve drawn above, the area enclosed by the disaster-damage curve and the horizontal (60–100 mm/h) and vertical (0–10%) boundaries was calculated, which indicates the urban resilience to short-term heavy rainfall.

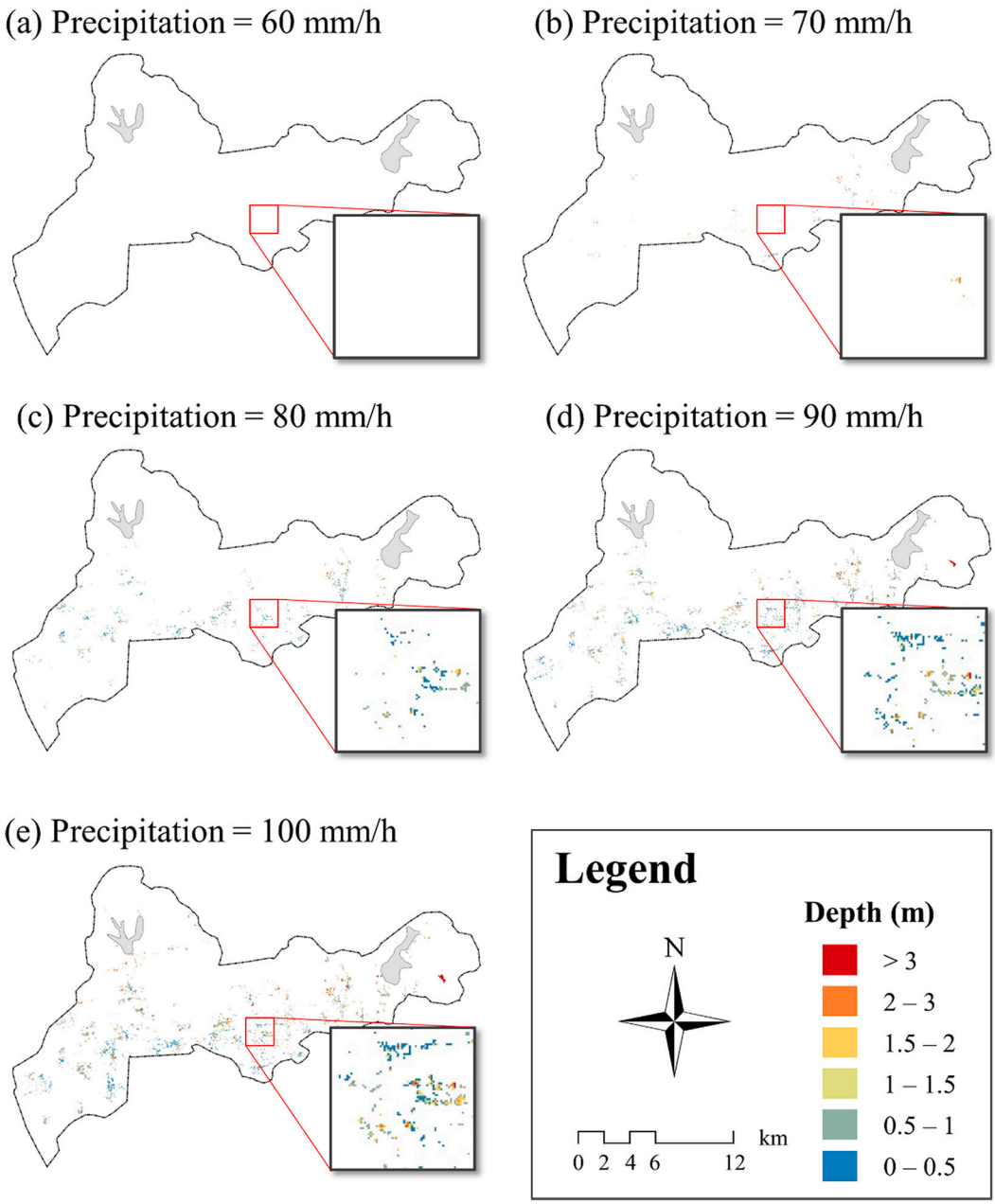

Fig. 6. Spatial distribution of the inundation area in the central urban area of Shenzhen in different rainfall scenarios from 60 to 100 mm/h. The inundation area and depth show an increasing trend with the increase of the precipitation intensity. Zoom-in portions of Shenzhen are displayed to present the change of inundation area and depth.

5. Results of the case study

5.1. Urban flooding simulation

The simulated flood maps are shown in Fig. 6. Under a series of rainfall scenarios, the inundation area presents an increasing trend with the increase of rainfall (Fig. 6). In the 60 mm/h rainfall scenario, only a few sporadic flooding points appear in the study area, and the inundation depth is also small, being between 0 and 0.5 m. It is because the capacity of drainage pipes is sufficient to cope with short-term heavy rainfall at this level without causing too much inundation. Along with the increase in rainfall, the inundation area continues to expand and reaches 7.17 km^2 at 100 mm/h, accounting for 2.21% of the total central urban area, and the inundation depth is mainly from 0 to 3 m, with a few areas above 3.5 m.

5.2. Disaster damage curve and resilience

By overlaying the simulated inundated area, inundated water depth, as well as the land-use types and their vulnerability in inundated areas, we estimated Shenzhen's damage rate in different rainfall scenarios and produced a disaster-damage curve (Fig. 7). As shown in Fig. 7, in the 60 mm/h rainfall scenario, the damage rate is very low, which is less than 0.01%. With the increase of rainfall from 60 to 100 mm/h, the disaster damage presents a monotone increase. In the 100 mm/h rainfall scenario, the damage rate reaches its maximum level at 9.65%.

As shown in Fig. 7, the damage rate increases from less than 0.01% to nearly 10% as the rainfall intensity grows from 60 mm/h to 100 mm/h. If we set the upper boundary of the damage rate as 10%, the relative resilience can be represented by the size of the shaded area which is 54% of the assessed disaster-damage space (x: 60–100 mm/h; y: 0–10%).

6. Discussions

6.1. Strategies to improve urban resilience

Improving resilience is one of the ultimate goals for sustainable development in cities. However, at present, resilient city building is still in the exploration stage. Although some cities and researchers have consciously proposed a series of measures to enhance resilience (Doyle et al., 2017; Pfefferbaum et al., 2018), most of them tend to formulate policies and guidelines from the macroscopic aspect without analysing or testing the effectiveness and applicability of the resilience improvement measures. In this sub-section, we demonstrate how we can use this proposed framework to analyse and compare strategies of building urban resilience to flooding in two examples.

The first strategy is to transform transportation land into permeable pavement. Waterlogging can be mitigated by engineering and technical means to reduce the pressure of drainage and modification of drainage systems with storage seepage measures at the waterhead. For example, green infrastructure (e.g., green roof, sunken green space, permeable pavement) widely discussed in recent years can alleviate urban flooding by maintaining water balance, and it is considered to be one of the most effective ways to improve the urban ecological environment (Lee et al., 2021; Chen et al., 2021; Li et al., 2020). The porous pavement is a typical measure to control rainfall and flood resources by reducing the impermeable proportion of a city to regulate runoff (Kia et al., 2021; Hu et al.,

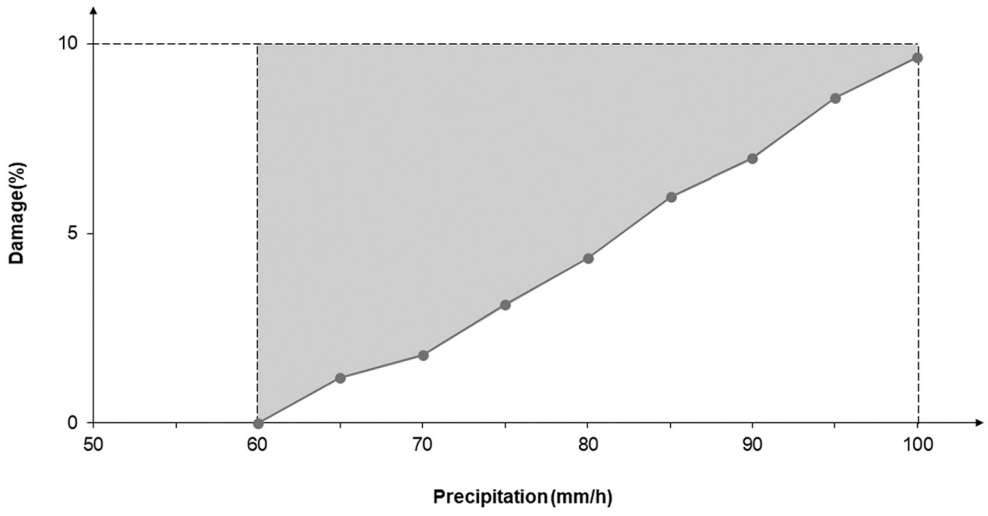

Fig. 7. Central Shenzhen's resilience to flooding. The shaded area indicates the central urban area of Shenzhen's relative resilience to urban flooding disaster.

2018; Park et al., 2020). It can cause acceleration of rainfall-runoff infiltration in the adjacent areas. Besides, it is a common method for stormwater regulation in roads or regions with inconvenient drainages.

The other strategy is to reduce the vulnerability of people and property exposed in disaster-stricken areas to decrease disaster damage. For example, in the Netherlands, about 1/3 of the land is below the sea level, and 65% is threatened by flooding. However, it has accumulated rich experience in water system planning, design, and urban flooding control. According to the depth-damage curves provided by the world database (Huizinga et al., 2017), the Netherlands has less vulnerable land in comparison to the same land use types in Asia, suggesting the Netherlands is more resilient to urban flooding.

Based on the above two strategies, two additional scenarios were set up: one was reconstruction of impermeable land for transportation, and the other was reduction of land vulnerability. Scenario simulations were carried out to evaluate the improvement of urban resilience under different strategies. In the permeable pavement scenario, we assumed that construction intensity of the pervious pavement in the study area was regarded as 100%, that is, all transportation land in Shenzhen was transformed into permeable pavement. The results showed that the relative resilience of Shenzhen can be increased by 18.5% from 54.0% to 64.0% after the transformation (Scenario 1 in Fig. 8). In the scenario of reducing vulnerability, it was assumed that China's capacity of disaster prevention and mitigation was improved to the Dutch standard, that is, the vulnerability of various land use types is reduced, and urban resilience is improved by 6.9% from 54.0% to 57.8% (Scenario 2 in Fig. 8).

The simulations showed that both strategies can improve Shenzhen's urban resilience to flooding to certain degrees, and the pavement transformation strategy was more effective in increasing resilience than the vulnerability reduction strategy in the given conditions. In Scenario 1, the construction of permeable pavements improved resilience by moving the disaster-damage curve to the right, suggesting this solution provided similar improvements across all disaster intensity conditions. In contrast, in Scenario 2, the vulnerability reduction elevated resilience by decreasing the slope of the curve, suggesting it was more effective when the disaster was more intensive. Although these two hypothetical scenarios are unlikely to happen in reality because of the extreme conditions set in this study (i.e., all transportation land is transformed, and the vulnerability of all land is reduced), they show how different resilience building strategies can be analysed, compared, and adapted in local contexts (e.g., Shenzhen in this case) under the framework proposed in this study.

In addition to these engineering-based strategies, attention should be paid to improving the ability of urban disaster prevention by optimising urban risk management before, during and after disasters. For example, establishing disaster early-warning systems needs more attention to minimise damages under extreme disasters and emergencies (Hofmann and Schüttrumpf, 2020; Acosta-Coll et al., 2018). Moreover, more studies are needed for the comprehensive risk identification and vulnerability assessment of urban security. During disasters, we should pay attention to minimising disaster risks with proactive responses and reducing the exposure of people and assets in affected areas (Schaer and Nygaard, 2016; Johann and Leismann, 2017; Rana et al., 2021). Moreover, we should consciously reduce the vulnerability of prone areas, enhance their ability to resist disasters, focus on the research of key technologies and equipment, such as the rapid recovery of urban systems after disasters, and reduce the damage caused by disasters (Ikeda et al., 2008; Wu et al., 2020; Chen et al., 2018).

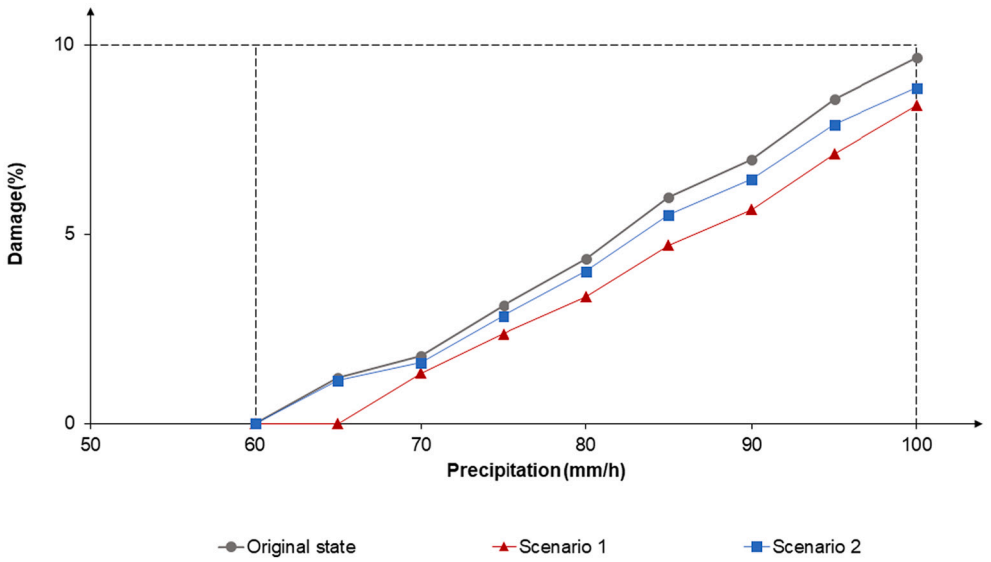

Fig. 8. Comparison between disaster damage curves of different resilience improvement strategies. Original state shows the disaster-damage relationship in the original scenario. Scenario 1 (red line) describes the disaster-damage relationship when all transportation land in Shenzhen is transformed into permeable pavement. The disaster damage curve (blue line) in Scenario 2 shows the effect of reducing vulnerability to urban flooding. (For interpretation of the references to colour in this figure legend, the reader is referred to the web version of this article.)

6.2. Features of the disaster-damage-based resilience assessment framework

According to the previous review of existing resilience assessment methods, most conventional resilience assessment methods are based on subsystem attributes, subjective understanding of resilience, or single events - an evaluation system is formed by selecting indicators and factors that can describe the state of resilience from natural, economic, social, and cultural perspectives (Brown et al., 2018; Yang et al., 2020), or from different management stages, such as prevention, response, recovery, and adaptation (Ouyang et al., 2012; Zhang et al., 2021). As discussed in the introduction, many of these approaches do not always support cross-region comparison of resilience or assessment of resilience building practices.

This study proposes a conceptual framework of quantitative resilience assessment based on the relationship between disaster and damage. The case study demonstrates the usability and extensibility of the framework. In addition, it provides an example of how the framework can be used to support urban flood management in general and a case reference for quantitative resilience assessment of other types of disasters in other areas. This general assessment approach is promising to enable intercomparisons of resilience across regions, which will be tested with empirical data by applying the framework to multiple cities as future work. Moreover, operational plans for resilience building can also be analysed and tested based on the framework.

6.3. Research uncertainties and future opportunities

This study simulated the spatial distribution and inundation depth of urban flooding, overlaid land use in the inundated areas and the vulnerability of different types of land, estimated the disaster damage rate of Shenzhen in different rainfall scenarios, and quantitatively evaluated the urban resilience based on the disaster-damage curve. However, there are still uncertainties in the result, suggesting future research opportunities for assessing urban resilience to short-term heavy rainfall in at least two aspects: urban flooding simulation and disaster damage estimation.

The SCS model is a simple and efficient approach for simulating urban flooding. For example, this study used rainfall as the input and inundation area as the output, but it did not consider water loss in transportation. In addition, the local equal volume method was used to simulate the remittance charge, which determines the distribution of the waterlogging area mainly according to the terrain. Without considering the flow characteristics of water, it leads to a result that there will be no ponding in a relatively high terrain as long as it is not flooded as a whole in a local area. Although the SCS model is more than sufficient for the demonstrative purposes in this paper, in the future, the proposed resilience assessment framework can work with a more sophisticated and detailed hydrologic model that allows a comprehensive analysis of drainage systems to improve the simulation accuracy.

For disaster damage estimation, there is no ready-to-use database of flood damage in China, which has become an obstacle to urban flood damage assessment, emergency response, and post-disaster reconstruction. Therefore, it is necessary to collect data and build databases about the value and vulnerability (e.g., depth-damage curves) of buildings, infrastructure, human society, economy, and other prone areas in each city, to improve the level of urban natural disaster risk assessment and provide a scientific basis for decision making of disaster prevention and reduction. For example, due to the lack of relevant data, we alternatively used the night-time light data as a proxy of the spatial distribution of land value in Shenzhen. It introduced uncertainties to the analysis because of its low spatial resolution (500 m), data noise, temporary lighting, and lighting spillover. In addition, the impact of urban flooding on humans (e.g., health and life damage), ecosystems, systemic risks, and long-term risks can also be considered in more holistic resilience assessments in the future. Therefore, we should pay more attention to building datasets of disaster damage and impact to support future resilience building and disaster management.

7. Conclusions

This study proposed and tested a disaster-damage-based framework for quantitatively assessing resilience based on the relationship between disaster intensity and damage. This framework provides an effective, intuitive, and widely applicable approach for quantitatively assessing resilience. At the same time, it is a useful tool for exploring resilience enhancement means and solutions. For example, we can optimise the disaster-damage curve to improve resilience using not only engineering, but also technical, social, ecological, or governance approaches, and compare the efficiency and effectiveness of different strategies to resilience enhancement. In this paper, we used Shenzhen as a study case to evaluate its urban resilience to flooding induced by short-term heavy rainfall and demonstrate the main features of the proposed framework by using it to analyse two resilience building strategies. Finally, we emphasise the importance of building global urban resilience databases to support more accurate, comprehensive, and comparable assessment of urban resilience to short-term heavy rainfall.

CRediT authorship contribution statement

Xiwen Zhang: Conceptualization, Investigation, Formal analysis, Writing – original draft, Writing – review & editing, Visualization. **Feng Mao:** Conceptualization, Investigation, Writing – review & editing, Visualization, Supervision. **Zhaoya Gong:** Investigation, Writing – review & editing, Supervision. **David M. Hannah:** Supervision, Writing - review & editing. **Yunnan Cai:** Writing – review & editing. **Jiansheng Wu:** Writing – review & editing.

Declaration of Competing Interest

The authors declare that they have no known competing financial interests or personal relationships that could have appeared to influence the work reported in this paper.

Data availability

Data will be made available on request.

Acknowledgements

We acknowledge the support from the National Natural Science Foundation of China Youth Science Fund (42101273).

References

Acosta-Coll, M., Ballester-Merelo, F., Martinez-Peiro, M., De la Hoz-Franco, E., 2018. Real-time early warning system design for pluvial flash floods—a review. Sensors. 18 (7), 2255. https://doi.org/10.3390/s18072255.
Adger, W.N., Hughes, T.P., Folke, C., Carpenter, S.R., RockstrOm, J., 2005. Social-ecological resilience to coastal disasters. Science. 309, 1036–1039.
Agnihotri, J., Mishra, S., 2021. Indian Economy and Nighttime Lights.
ARUP, 2015. Climate Risk and Adaption Framework and Taxonomy, CRAFT[EB/OL]. https://data.bloomberglp.com/mayors/sites/14/2015/06/C40-CRAFT_comms-brochure-final.pdf.
Bayazit, Y., Koc, C., Bakis, R., 2020. Urbanization impacts on flash urban floods in Bodrum Province, Turkey. Hydrol. Sci. J. 66 (1), 118–133.
Birkmann, J., 2006. Measuring vulnerability to promote disaster-resilient societies: conceptual frameworks and definitions. In: Birkmann, J. (Ed.), Measuring Vulnerability to Natural Hazards: Towards Disaster Resilient Societies, Vol. 01. United Nations University Press, New York, pp. 9–54.
Bozza, A., Asprone, D., Fabbrocino, F., 2017. Urban resilience: a civil engineering perspective. Sustainability 9, 103.
Brown, N.A., Orchiston, C., Rovins, J.E., Feldmann-Jensen, S., Johnston, D., 2018. An integrative framework for investigating disaster resilience within the hotel sector. J. Hosp. Tour. Manag. 36, 67–75.
Bruneau, M., Chang, S.E., Eguchi, R.T., Lee, G.C., O'Rourke, T.D., Reinhorn, A.M., Shinozuka, M., Tierney, K., Wallace, W.A., von Winterfeldt, D., 2003. A framework to quantitatively assess and enhance the seismic resilience of communities. Earthquake Spectra 19 (4), 733–752.
Chen, P., Zhang, J., Sun, Y., 2018. Research on emergency rescue of urban flood disaster based on wargame simulation. J. Indian Soc. Remote Sens. 46 (10), 1677–1687.
Chen, C.K., Xu, L.L., Zhao, D.Y., Xu, T., Lei, P., 2020a. A new model for describing the urban resilience considering adaptability, resistance and recovery. Saf. Sci. 128, 104756.
Burton, P., Tiernan, A., Wolski, M., Drennan, L., Morrissey, L., 2019. Resilient cities, user-driven planning, and open data policy. In: Hawken, S., Han, H., Pettit, C. (Eds.), Open Cities | Open Data. Palgrave Macmillan, Singapore. https://doi.org/10.1007/978-981-13-6605-5_17.
Chen, F., Jia, H.C., Zhang, C.R., 2020b. A comprehensive method for evaluating marine disaster risk reduction capacity in China. Sustainability. 12 (3), 825. https://doi.org/10.3390/su12030825.
Chen, W.J., Wang, W.Q., Huang, G.R., Wang, Z.L., Lai, C.G., Yang, Z.Y., 2021. The capacity of grey infrastructure in urban flood management: a comprehensive analysis of grey infrastructure and the green-grey approach. Int. J. Disaster Risk Reduction 54, 102045.
Cheng, Y., Elsayed, E.A., Huang, Z., 2022. Systems resilience assessments: a review, framework and metrics. Int. J. Prod. Res. 60 (2), 595–622.
Chi, J., Jiao, L., Dong, T., Gu, Y., Ma, Y., 2016. Quantitative identification and visualization of urban functional area based on POI data. J. Geom. 41, 68–73.
Cimellaro, G.P., Reinhorn, A.M., Bruneau, M., 2010. Seismic resilience of a hospital system. Struct. Infrastruct. Eng. 6 (1–2), 127–144.
Cochrane, H.C., 2004. Indirect damage from natural disasters: measurement and myth. In: Okuyama, Y., Chang, S.E. (Eds.), Modeling Spatial and Economic Impacts of Disasters. Advances in Spatial Science. Springer, Berlin, Heidelberg. https://doi.org/10.1007/978-3-540-24787-6_3.
Cutter, S.L., Derakhshan, S., 2018. Temporal and spatial change in disaster resilience in us counties, 2010–2015. Environ. Hazards 19, 10–29.
Cutter, S.L., Barnes, L., Berry, M., et al., 2008. A place-based model for understanding community resilience to natural disasters. Glob. Environ. Chang. 18 (4), 598–606.
De Groeve, T., Annunziato, A., Vernaccini, L., 2013. Overview of Disaster Risks that the EU Faces. JRC Scientific and Policy Reports; European Commission; Joint Research Centre, Ispra, Italy.
Dessavre, D.G., Ramirez, J.E., Barker, K., 2016. Multidimensional approach to complex system resilience analysis. Reliab. Eng. Syst. Saf. 149, 34–43.
Doll, C.N.H., Muller, J.P., Morley, J.G., 2006. Mapping regional economic activity from night-time light satellite imagery. Ecol. Econ. 57, 75–92.
Doyle, A., Hynes, W., Purcell, S.M., Rochford, M., 2017. Exploring the role of planning in urban resilience enhancement—an irish perspective. In: Fekete, A., Fiedrich, F. (Eds.), Urban Disaster Resilience and Security. The Urban Book Series, Springer, Cham. https://doi.org/10.1007/978-3-319-68606-6_3.
Evans, J.P., 2011. Resilience, ecology and adaptation in the experimental city. Trans. Inst. Br. Geogr. 36, 223–237.
FEMA/NIBS, 2015. Multi-hazard Damage Estimation Methodology Eathquake Model (Hazus-MH 2.1). Washington, D.C.
Feofilovs, M., Romagnoli, F., 2020. Assessment of urban resilience to natural disasters with a system dynamics tool: case study of latvian municipality. Environmen. Climate Technol. 24 (3), 249–264.
Field, C., Barros, V., Stocker, T., Qin, D., 2012. In: *Managing the risks of extreme events and disasters to advance climate change adaptation: A Special Report of Working Groups I and II of the Intergovernmental Panel on Climate Change*. Cambridge University Press, Cambridge. https://doi.org/10.1017/CBO9781139177245.
Gall, M., 2015. The suitability of disaster damage databases to measure damage and damage from climate change. Int. J. Global Warm. 8 (2), 170–190.
Gasser, P., Lustenberger, P., Cinelli, M., Matteo Spada, W.K., Burgherr, P., Hirschberg, S., Stojadinovic, B., Sun, Y.T., 2021. A review on resilience assessment of energy systems. Renew. Sust. Energ. Rev. 6 (5), 273–299.
Hajibabaee, M., Amini-Hosseini, K., Ghayamghamian, M.R., 2014. Earthquake risk assessment in urban fabrics based on physical, socioeconomic and response capacity parameters (a case study: Tehran city). Nat. Hazards 74, 2229–2250.
Henderson, J.V., Storeygard, A., Weil, D.N., 2012. Measuring economic growth from outer space. Am. Econ. Rev. 102, 994–1028.
Henry, D., Ramirez-Marquez, J.E., 2012. Generic metrics and quantitative approaches for system resilience as a function of time. Reliab. Eng. Syst. Saf. 99, 114–122.
Hernantes, J., Labaka, L., Turoff, M., Hiltz, S.R., Bañuls, V.A., 2017. Moving forward to disaster resilience: perspectives on increasing resilience for future disasters. Technol. Forecast Soc. Change 121, 1–6.
Hofmann, J., Schüttrumpf, H., 2020. Risk-based and hydrodynamic pluvial flood forecasts in real time. Water. 12 (7), 1895.
Hosseini, S., Barker, K., 2016. Modeling infrastructure resilience using bayesian networks: a case study of inland waterway ports. Comput. Ind. Eng. 93, 252–266.
Hosseini, S., Al Khaled, A., Sarder, M.D.A., 2016. General framework for assessing system resilience using bayesian networks: a case study of sulfuric acid manufacturer. J. Manuf. Syst. 41, 211–227.
Hu, M.C., Zhang, X.Q., Siu, Y.L., Li, Y., Tanaka, K., Yang, H., Xu, Y.P., 2018. Flood mitigation by permeable pavements in chinese sponge city construction. Water. 10 (2), 172. https://doi.org/10.3390/w10020172.

Huizinga, J., Moel, H., Szewczyk, W., 2017. Global Flood Depth-damage Functions: Methodology and the Database with Guidelines. https://doi.org/10.2760/16510. EUR 28552 EN.
Ikeda, S., Sato, T., Fukuzono, T., 2008. Towards an integrated management framework for emerging disaster risks in Japan. Nat. Hazards 44 (2), 267–280.
Irwin, E.G., Jayaprakash, C., Munroe, D.K., 2009. Towards a comprehensive framework for modeling urban spatial dynamics. Landsc. Ecol. 24 (9), 1223–1236.
Jabareen, Y., 2013. Planning the resilient city: concepts and strategies for coping with climate change and environmental risk. Cities 31, 220–229. https://doi.org/10.1016/j.cities.2012.05.004.
Jahan, K., Pradhanang, S.M., Bhuiyan, M.A.E., 2021. Surface runoff responses to suburban growth: an integration of remote sensing, GIS, and curve number. Land 10.
Jasinski, T., 2019. Modeling electricity consumption using nighttime light images and artificial neural networks. Energy 179 (15), 831–842.
Jia, W.A., Jlab, C., Hao, W.A., et al., 2020. Matching analysis of investment structure and urban inundation control function of sponge cities in China. J. Clean. Prod. 266.
Jin, S.F., Wang, L.X., Yan, X.D., 2020. Physics and chemistry of the Earth. Parts A/B/C 120, 102920.
Johann, G., Leismann, M., 2017. How to realise flood risk management plans efficiently in an urban area – the seseke project. J. Flood Risk Manag. 10 (2), 173–181.
Kabir, M.H., Sato, M., Habbiba, U., Bin Yousuf, T., 2018. Assessment of urban disaster resilience in Dhaka North City Corporation (DNCC), Bangladesh. Proc. Eng. 212, 1107–1114.
Keating, A., Campbell, K., Mechler, R., Magnuszewski, P., Mochizuki, J., Liu, W., et al., 2017. Disaster resilience: what it is and how it can engender a meaningful change in development policy. Dev. Policy Rev. 35 (1), 65–91.
Kia, A., Delens, J.M., Wang, H.S., Cheeseman, C.R., 2021. Structural and hydrological design of permeable concrete pavements. Case Stud. Construct. Mater. 15. https://doi.org/10.1016/j.cscm.2021.e00564.
Lee, Dae Woong, 2019. Local Government's disaster management capacity and disaster resilience. Local Gov. Stud. 2, 1–24.
Lee, H., Song, K., Kim, G., Chon, J., 2021. Flood-adaptive green infrastructure planning for urban resilience. Landsc. Ecol. Eng. 17, 427–437.
Leichenko, R., 2012. Climate change, globalization, and the double exposure challenge to sustainability: rolling the dice in coastal New Jersey. Springer, New York.
Li, X., Xu, H., Chen, X., Li, C., 2013. Potential of NPP-VIIRS nighttime light imagery for modeling the regional economy of china. Remote Sens. 5, 3057–3081.
Li, L., Chan, P.W., Wang, D.L., Tan, M.Y., 2015. Rapid urbanization effect on local climate: intercomparison of climate trends in Shenzhen and Hong Kong, 1968–2013. Clim. Res. 63 (2), 145–155.
Li, L.Y., Uyttenhovea, P., Vaneetvelde, V., 2020. Planning green infrastructure to mitigate urban surface water flooding risk –a methodology to identify priority areas applied in the city of Ghent. Landsc. Urban Plan. 194, 103703. https://doi.org/10.1016/j.landurbplan.2019.103703.
Manyena, S.B., O'Bein, G., O'Keefe, P., Rose, J., 2011. Disaster resilience: a bounce back or bounce forward ability? Local Environ. 16 (5), 417–424.
Mao, F., Clark, J., Karpouzoglou, T., Dewulf, A., Buytaert, W., Hannah, D., 2017. HESS Opinions: A conceptual framework for assessing socio-hydrological resilience under change. Hydrol. Earth Syst. Sci. 21 (7), 3655–3670. https://doi.org/10.5194/hess-21-3655-2017.
McLellan, B., Zhang, Q., Farzaneh, H., Utama, A.N., Ishihara, K.N., 2012. Resilience, sustainability and risk management: a focus on energy. Challenges. 3 (2), 153–182.
Meyer, V., Scheuer, S., Haase, D., 2009. A multicriteria approach for flood risk mapping exemplified at the Mulde River, Germany. Nat. Hazards 48 (1), 17–39.
Ministry of Housing and Urban-Rural Development of the People''s Republic of China, 2014. Technical Guidelines for Sponge City Construction- Construction of Stormwater Systems for Low Impact Development.
Ministry of Housing and Urban-Rural Development of the People''s Republic of China (MOHURD), 2016. Code for Design of Outdoor Wastewater Engineering (GB 50014–2006).
Mugume, S.N., Gomez, D.E., Fu, G., Farmani, R., Butler, D., 2015. A global analysis approach for investigating structural resilience in urban drainage systems. Water Res. 81, 15–26.
Munawar, H.S., Khan, S., Anum, N., Qadir, Z., Kouzani, A.Z., 2021. Post-flood risk management and resilience building practices: a case study. Appl. Sci. 11 (11), 4823.
Murdock, H.J., De Bruijn, K.M., Gersonius, B., 2018. Assessment of critical infrastructure resilience to flooding using a response curve approach. Sustainability. 10 (10), 3470.
Mustafa, A., Bruwier, M., Archambeau, P., Erpicum, S., Pirotton, M., Dewals, B., Teller, J., 2018. Effects of spatial planning on future flood risks in urban environments. J. Environ. Manag. 225 (1), 193–204.
Nan, C., Sansavini, G., 2017. A quantitative method for assessing resilience of interdependent infrastructures. Reliab. Eng. Syst. Saf. 157, 35–53.
Nelson, D.R., Adger, W.N., Brown, K., 2007. Adaptation to environmental change: contributions of a resilience framework. Annu. Rev. Environ. Resour. 32 (1), 395–419.
Newman, P., Beatley, T., Boyer, H., 2009. Resilient Cities: Responding to Peak Oil and Climate Change. Island Press, Washington, DC, USA.
NHERI, 2018. SIMCENTER[EB/OL]. https://simcenter.designsafe-ci.org/. https://simcenter.designsafe-ci.org/.
Nunes, D.M., Tom'e, A., Pinheiro, M.D., 2019. Urban-centric resilience in search of theoretical stabilisation? A phased thematic and conceptual review. J. Environ. Manag. 282–292.
Nurbandi, W., Prasetya, R., Kamal, M., 2018. The Relationship Between Artificial Nighttime Light (ANTL) and Built-Up Area: a Remote Sensing Perspective[C]// 2018 4th International Conference on Science and Technology (ICST).
Odum, H.T., Odum, E.C., 1976. Energy Basis for Man and Nature. McGraw-Hill, New York.
Ongkowijoyo, C.S., Doloi, H., 2018. Risk-based resilience assessment model focusing on urban infrastructure system restoration. Procedia Eng. 212, 1115–1122.
Ouyang, M., Dueñas-Osorio, L., Min, X., 2012. A three-stage resilience analysis framework for urban infrastructure systems. Struct. Saf. 36–37, 23–31.
Park, J., Park, J., Cheon, J., Lee, J., Shin, H., 2020. Analysis of infiltrating water characteristics of permeable pavements in a parking lot at full scale. Water. 12, 2081.
Pfefferbaum, B., Van Horn, R.L., Pfefferbaum, R.L., 2018. Involving adolescents in building community resilience for disasters. Adolesc. Psychiatry 7 (4), 253–265.
Polin, C.R., Kane, M.B., 2021. The effect of time-varying value on infrastructure resilience assessments. IEEE Access. 9, 134556–134575.
Rana, I.A., Asim, M., Aslam, A.B., Jamshed, A., 2021. Disaster management cycle and its application for flood risk reduction in urban areas of Pakistan. Urban Clim. 38, 100893 https://doi.org/10.1016/j.uclim.2021.100893.
Reed, D.A., Kapur, K.C., Christie, R.D., 2009. Methodology for assessing the resilience of networked infrastructure. IEEE Syst. J. 3 (2), 174–180.
Restrepo, J.D.C., Morales-Pinzon, T., 2018. Urban metabolism and sustainability: precedents, genesis and research perspectives. Resour. Conserv. Recycl. 131, 216–224.
Rockefeller Foundation, ARUP. City Resilience Framework. 2014. Http://publications.Arup.com/Publications/C/City_Resilience_Framework.asp.
Saja, A.M.A., Goonetilleke, A., Teo, M., et al., 2019. A critical review of social resilience assessment frameworks in disaster management. Int. J. Disaster Risk Reduction 35, 101096.
Sajjad, M., Chan, J., Chopra, S.S., 2021. Rethinking disaster resilience in high-density cities: towards an urban resilience knowledge system. Sustain. Cities Soc. 69, 102850.
Sapountzaki, K., 2012. Vulnerability management by means of resilience. Nat. Hazards 60, 1267–1285. https://doi.org/10.1007/s11069-011-9908-3.
SAVI, 2020. How savi works[EB/OL]. https://iisd.org/savi/how-savi-works/.
Schaer, C., Nygaard, I., 2016. Flood management in urban senegal: an actor-oriented perspective on national and transnational adaptation interventions. Clim. Dev. 10, 243–258.
Serre, D., Barroca, B., 2013. Preface "Natural hazard resilient cities". Nat. Hazards Earth Syst. Sci. 13 (10), 2675–2678.
Sharifi, A., Yamagata, Y., 2016. Principles and criteria for assessing urban energy resilience: a literature review. Renew. Sust. Energ. Rev. 60, 1654–1677.
SIM·CI, 2018. Sim·CI Simulation platform[EB/OL]. https://sim-ci.com/ (2018)[2020-05-11]. https://sim-ci.com/en/simulation-platform/.
STAR COMMUNITIES, 2020. CERTIFIED STAR COMMUNITIES[EB/OL]. http://www.starcommunities.org/. http://www.starcommunities.org/certification/certified-star-communities/.

Sun, J., Di, L., Sun, Z.H., Wang, J.Y., Wu, Y.D., 2020. Estimation of GDP using deep learning with NPP-VIIRS imagery and land cover data at the county-level in CONUS. IEEE J. Select. Topics Appl. Earth Observ. Remote Sens. 99.
Sun, Y., Wang, S., Zhang, X., et al., 2021. Estimating local-scale domestic electricity energy consumption using demographic, nighttime light imagery and twitter data. Energy 12, 120351.
Sutton, P.C., Elvidge, C.D., Ghosh, T., 2007. Estimation of gross domestic product at sub-national scales using nighttime satellite imagery. Int. J. Ecol. Econ. Stat. 8, 5–21.
Tanner, T., Bahadur, A., Moench, M., 2017. Challenges for Resilience Policy and Practice. Available online: https://www.odi.org/sites/odi.org.uk/files/resource-documents/11733.pdf (accessed on 20 September 2020).
Thryse, C., Arnbjerg-Nielsen, K., Borup, M., 2018. Identifying fit-for-purpose lumped surrogate models for large urban drainage systems using GLUE. J. Hydrol. 568.
Tian, X., Li, D., Zhou, J., Zhou, Y., Zhang, Z., 2019. Characteristics analysis on short-time heavy rainfall during the flood season in Shanxi Province, China. J. Geosci. Environ. Protect. 7 (3), 190–203.
Timmerman, P., 1981. Vulnerability, resilience and the collapse of society: a review of models and possible climatic applications. Canada University of Toronto, Toronto.
Tiwari, K., Goyal, R., Sarkar, A., 2018. GIS-based methodology for identification of suitable locations for rainwater harvesting structures. Water Resour. Manag. 32, 1811–1825.
Tong, P., 2021. Characteristics, dimensions and methods of current assessment for urban resilience to climate-related disasters: a systematic review of the literature. Int. J. Disaster Risk Reduction 60, 102276.
Tyler, S., Moench, M., 2012. A framework for urban climate resilience. Clim. Dev. 4 (4), 311–326.
UNFCCC, 2012. A Literature Review on the Topics in the Context of Thematic Area 2 of the Work Programme on Damage and Damage: A Range of Approaches to Address Damage and Damage Associated with the Adverse Effects of Climate Change (FCCC/SBI/2012/INF.14).
United Nations Office for Disaster Risk Reduction, 2009. 2009 UNISDR Terminology on Disaster Risk Reduction, Geneva (ISBN 978–600-6937-11-3).
United States Department of Agriculture, 1986. Urban Hydrology for Small Watersheds Technical Release 55 (TR-55). Natural Resources Conservation Service. https://www.nrcs.usda.gov/Internet/FSE_DOCUMENTS/stelprdb1044171.pdf.
Vachette, A., 2017. Integrating Disaster Risk Reduction and Climate Change Adaptation in Vanuatu: The Art and Practice of Building Resilience to Hazards. Springer International Publishing.
Verma, S., Mishra, S.K., Verma, R.K., 2020. Improved runoff curve numbers for a large number of watersheds of the usa improved runoff curve numbers for a large number of watersheds of the USA. Hydrol. Sci. J. 65, 16. https://doi.org/10.1080/02626667.2020.1832676.
Verma, R.K., Verma, S., Mishra, S.K., Pandey, A., 2021. SCS-CN-based improved models for direct surface runoff estimation from large rainfall events. Water Resour. Manag. 1–27.
Vugrin, E.D., Warren, D.E., Ehlen, M.A., 2011. A resilience assessment framework for infrastructure and economic systems: quantitative and qualitative resilience analysis of petrochemical supply chains to A Hurricane. Process. Saf. Prog. 30, 280–290.
Watson, I., 2016. Resilience and disaster Risk Reduction: Reclassifying Diversity and National Identity in Post-earthquake Nepal. Third World Q. 483–504.
Wilkinson, C., 2021. Urban resilience: what does it mean in planning practice? Plan. Theory Pract. 13, 319–324.
World Bank Group, 2015. City Strength Diagnostic: Methodological Guidebook, pp. 1–194.
Wu, Z., Shen, Y., Wang, H., et al., 2020. An ontology-based framework for heterogeneous data management and its application for urban flood disasters. Earth Sci. Inf. 13 (2), 377–390.
Xiao, B., Wang, Q.H., Jun, F., Han, F.P., 2011. Application of the SCS-CN model to runoff estimation in a small watershed with high spatial heterogeneity. Pedosphere. 21 (6), 738–749.
Xu, J., Yang, F., 2017. A study of urban functional area identification methods based on big data of social sensing. Urban Architect. 9, 30–34.
Yamagishi, H., Doshida, S., Pimiento, E., 2013. GIS analysis of heavy-rainfall induced shallow landslides in Japan. In: *Landslide Science and Practice*. Springer, Berlin, Heidelberg, pp. 601–607.
Yang, Y., Li, Y., Chen, F., Zhang, S., Hou, H., 2019. Regime shift and redevelopment of a mining area's socio-ecological system under resilience thinking: a case study in Shanxi Province, China. Environ. Dev. Sustain. 21, 2577–2598.
Yang, Y.Y., Guo, H.X., Chen, L.F., Liu, X., Gu, M.Y., Pan, W.W., 2020. Multiattribute decision making for the assessment of disaster resilience in the three gorges reservoir area. Ecol. Soc. 25, 2. https://doi.org/10.5751/ES-11464-250205.
Yang, B., Wang, Y., Nan, S., 2021. Joint influence of anomalous medium-and small-scale circulations on short-term heavy rainfall events over Beijing. Int. J. Climatol. 41.
Zhang, J., Zhang, M., Li, G., 2021. Multi-stage composition of urban resilience and the influence of pre-disaster urban functionality on urban resilience. Nat. Hazards 2.
Zhou, Q.Q., Luo, J.H., Su, J.H., Yi, R., 2021. Impacts of changing drainage indicators on urban flood volumes in historical urbanization in the case of Northern China. Urban Water J. 22, 1–12.